Journal of Magnetic Resonance 194 (2008) 81–88

Contents lists available at ScienceDirect

Journal of Magnetic Resonance

journal homepage: www.elsevier.com/locate/jmr

Improved *J*-compensated sequences based on short composite pulses

A.M. Torres [a,*], W.A. Bubb [b], D.J. Philp [c], P.W. Kuchel [b]

[a] Nanoscale Organisation and Dynamics Group, College of Health and Science, University of Western Sydney, Penrith South DC, NSW 1797, Australia
[b] School of Molecular and Microbial Biosciences, University of Sydney, NSW 2006, Australia
[c] National Centre for Epidemiology and Population Health, Australian National University, Canberra, ACT 0200, Australia

ARTICLE INFO

Article history:
Received 7 March 2008
Revised 30 May 2008
Available online 7 June 2008

Keywords:
J-compensation
Composite pulse
HMBC
LR-*J*-HSMQC
Pulse-sequence simulation
Mathematica
Spectral editing

ABSTRACT

Efficient *J*-compensated sequences that are shorter in duration and use less RF pulses have been created from short but very efficient composite 90° RF pulses. The improved *J*-compensation transforms in-phase into antiphase magnetization and can be incorporated in any pulse sequence that involves evolution of heteronuclear *J*-couplings. The compensated sequences were tested and incorporated into an HMBC sequence. *J*-compensated experiments referred to as HMBC-*J*45 + 90A and HMBC-*J*45 + 90B, were found to be effective over a wide range of *J* values.

1. Introduction

Composite pulses, used either for spin–spin decoupling or as a replacement for an inefficient or imprecise single radiofrequency (RF) pulse [1,2], are indispensable tools in NMR. These special types of pulses consist of a series of two or more phase-shifted RF pulses designed to eliminate, or lessen to a significant extent, inadequacies in a single RF pulse, including sensitivity to B_1-field inhomogeneity, pulse miscalibration, and resonance-offset effects. Many varieties of composite pulses, ranging from the popular and relatively simple $90_0180_{90}90_0$ composite 180° pulse [2], to the more sophisticated BURP sequences [3], have been developed.

One useful application of composite pulses is that they serve as templates for creating compensated pulse sequences that are less sensitive to variations in spin–spin coupling constants, *J*, present in a given molecular system [4–7]. These methods, commonly referred to as *J*-compensated sequences, make conventional magnetization-detection sequences more effective over a wide range of *J*-coupling constants. Examples of experiments that have been studied for *J*-compensation include cross-polarization (CP) [8], double-quantum excitation [5], INEPT [4], APT [9,10], and HSQC [11].

The biggest drawback of many *J*-compensated experiments is that they incorporate more RF pulses and delays than the conventional experiments. This makes them longer in duration than conventional sequences and therefore more susceptible to signal loss through relaxation. Moreover, *J*-compensated sequences often require additional chemical shift refocusing pulses that render them extra prone to pulse-calibration imperfections. Here, we describe improved *J*-compensated sequences that have fewer pulses and shorter delays. First, we patterned these compensated sequences from short composites pulses of the form $(a\beta)_\phi(b\beta)_\varphi$ which have been tuned for *J*-compensation using the simulation program *Ptolemy* [12]. Wherever possible, the resulting compensated sequences are then manipulated further to decrease the number of RF pulses. These unconventional *J*-compensated sequences can be easily incorporated into other pulse sequences to lessen their sensitivity to the magnitude of *J*-coupling constants. As an example, we incorporated a number of the compensated sequences into the HMBC experiment and tested their performance using sodium acrylate as a model compound.

2. Theory

To shorten their duration, *J*-compensated RF pulse sequences are ideally patterned on short composite pulses. In this study, we concentrate on the *J*-compensated conversion of in-phase to antiphase magnetization by spin–spin coupling as applicable in HMBC, HMQC and INEPT experiments. This requires the use of a composite 90° pulse or more generally a composite β pulse (where $\beta = \gamma B_1 t$, γ is the magnetogyric ratio of the spin, B_1 is the amplitude of the RF field, and t is the pulse duration) for which the angle β is nominally set to 90°. The shortest composite pulse that can be used is a

* Corresponding author. Fax: +61 2 4620 3025.
E-mail address: a.torres@uws.edu.au (A.M. Torres).

1090-7807/$ - see front matter © 2008 Elsevier Inc. All rights reserved.
doi:10.1016/j.jmr.2008.06.001

two-step pulse train of the form $(a\beta)_{\phi}\ (b\beta)_{\varphi}$ where a and b correspond to coefficients of the first and second RF pulses with nominal magnitude β, while ϕ and φ denote the corresponding phases. The three most popular composite pulses of this form are the $\beta_0(2\beta)_{120}$ [13], $\beta_0(\beta)_{90}$ [1], and $\beta_0(2\beta)_{90}$ [14,15]. We aim to verify the efficiencies of these composite pulses and then make shorter variants for *J*-compensation by optimizing their efficiencies to create transverse magnetization Iy, Ix or Ixy (defined as total transverse magnetization, $\sqrt{(\mathrm{Ix})^2 + (\mathrm{Iy})^2}$) over a wide range of β values.

The optimization was implemented in the program *Ptolemy* by first determining the analytical mathematical expression for transverse magnetization, Ix and Iy, in terms of the four parameters a, b, ϕ, φ, and tip angle β. The efficiency term "η" was then set up as a summation of transverse magnetization Ix, Iy, or Ixy (depending on the requirement) over a range of specified β values in 1° steps. With the NMaximize function in *Mathematica*, the optimal set of values of the four parameters was obtained numerically by iteration, after constraining the coefficients a and b to specified limits.

2.1. Optimization of the conversion of Iz to −Iy

The $\beta_0(2\beta)_{120}$ composite pulse derived by Levitt et al. [13] was readily confirmed by *Ptolemy* optimization of −Iy since the equivalent $\beta_{-60}(2\beta)_{60}$ sequence was obtained after setting the effective β range to be between 70° and 110°, and the sum of pulse coefficients ($a + b$) to 3. The transverse magnetization profiles of the simple and various composite pulses for creation of transverse magnetization −Iy are presented in Fig. 1. The composite $\beta_0(2\beta)_{120}$ was used earlier in *J*-compensation of INEPT [4] and DEPT [7], however its duration was not desirable as it is 3 times longer than the regular sequence. A much shorter version $(0.5\beta)_{-60}(\beta)_{60}$ of the sequence was obtained by optimization when the center of the β range was set to 180° instead of 90°. Although this version is less effective for the β range near 90°, it is a potentially good candidate for use in *J*-compensated experiments as it is only 1.5 times longer than the regular pulse β and it is effective over a wider range of β values.

When the sum of the pulse coefficients ($a + b$) was limited to 1.5, and the effective β range was set between 70° and 110°, optimization yielded a short composite pulse of the form $(0.5\beta)_{45}(\beta)_{-45}$. This composite pulse is actually equivalent to a $\beta_0(2\beta)_{90}$ composite pulse that was introduced by Sorensen et al. [14,15], which was shown to be "perfect" in transforming Iz to transverse magnetization, Ix and Iy at $\beta = 45°$, 90°, 135°. Unlike $\beta_0(2\beta)_{120}$, however, the composite pulse $(0.5\beta)_{45}(\beta)_{-45}$ is only as efficient as the simple β_0 pulse for $\beta < 90°$ but it is substantially more efficient at higher β values, although it has a local minimum at $\beta = 180°$.

2.2. Optimization of the conversion of Iz to Ixy

Composite pulses that transform Iz to Ix and Iy may be useful in *J*-compensation of experiments, such as HMBC [16], HMQC [17] and D-HMBC [18], which use both antiphase magnetizations, 2IxSz and 2IySz, in producing the desired signal in one transient. Since the phase of the transverse magnetization created by the composite pulse is irrelevant in this case, it is convenient to fix ϕ, the phase of the first pulse, to zero during optimization and thus eliminate degenerate solutions wherein $|\phi - \varphi|$ are equal. The optimization procedure is similar to that implemented for the conversion of Iz to −Iy except that Ixy is used in the efficiency term, "η".

Unsurprisingly, optimization of signal for the β range 70–110° yields the composite pulse $(\beta)_0(2\beta)_{117}$, which is in essence equivalent to Levitt's $(\beta)_0(2\beta)_{120}$, when the upper limit to the sum of the coefficients a and b is made to be less than 5 (the difference between the two is likely due to linear approximation); setting the upper limit of the sum to 2 and 1.5, yields $(0.9\beta)_0(1.1\beta)_{89}$ and $(0.75\beta)_0(0.75\beta)_{80}$, respectively. Note that these composite pulses are basically the pulse train $(\beta)_0(\beta)_{90}$, introduced by Freeman et al. [1], and shown to be very efficient in creating transverse magnetization, Ixy.

A special group of short but unusually efficient composite 90° pulses for the creation of Ixy may be obtained by fixing the values of the parameters, a to 1, and ϕ to 0, and then numerically optimizing parameters b and φ over a range of high β values, starting from 60°. Composite pulses of the form $(\beta)_0(\mathrm{b}\beta)_{\varphi}$ will have the same efficiency as a simple β pulse for which β is nominally centered on 90°, plus bonus efficiency at β values greater than 90°. Such optimization for the creation of Ixy is possible in this case because, unlike that in the conversion to −Iy, the phase of the resulting transverse magnetization is not important in the numerical

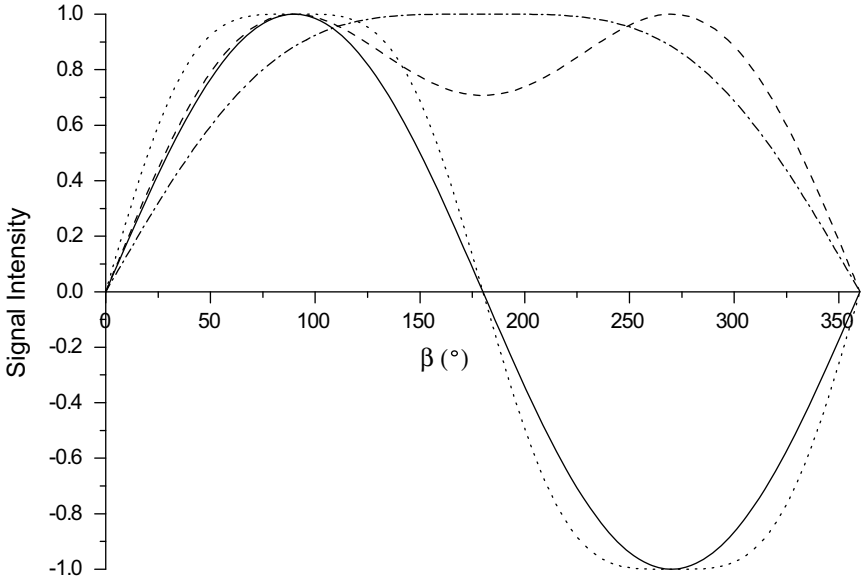

Fig. 1. −Iy magnetization profiles (relative signal intensity) of simple and optimized composite pulses. Simple β (solid line), $(\beta)_{-60}(2\beta)_{60}$ (dotted line), $(0.5\beta)_{-45}(\beta)_{45}$ (dashed line) and $(0.5\beta)_{-60}(\beta)_{60}$ (dotted dashed line).

optimization. *J*-compensated methods patterned from these composite pulses will be especially effective for high *J* values.

Fig. 2 presents short composite pulses $(\beta)_0(b\beta)_\varphi$ derived from optimization in the β range 60–520°. In general, the β range was increased as the coefficient *b* was reduced, while the phase of the second pulse φ remained relatively constant at 90°. Over the narrow β range of 60–120°, $(\beta)_0(\beta)_{90}$ provided the best performance (Fig. 2A). For the increased β range of 60–300°, a composite pulse of the form $(\beta)_0(0.5\beta)_{90}$ was optimal (Fig. 2B); for a β range of 60–360°, the "best" composite pulse had the form $(\beta)_0(0.33\beta)_{90}$ (Fig. 2C). Further reduction of the coefficient *b* to 0.25 increased the range of β to 520° (Fig. 2D).

Prior to this study, *J*-compensated APT [9], *J*-HSMQC [11] and LR-*J*-HSMQC [19] had already employed compensated sequences that were implicitly patterned on a composite pulse of the form $(\beta)_0\,(b\beta)_{90}$. It was shown then that *b* values of 0.5 and 0.33 would yield more favorable spectral profiles than a *b* value of 1.0, however these values were obtained empirically and not by numerical optimization. Here, we establish unequivocally that these values are indeed optimal and that this type of composite pulse may be made more effective over a wider range of β values by further decreasing *b* to 0.25 and even 0.20 (not shown). This could potentially lead to better *J*-compensated APT and "HSQC like" experiments.

A study of the efficiency of the short composite pulses of the form $(\beta)_0(b\beta)_{90}$ as shown in Fig. 2 revealed that although reducing the value of the *b* coefficient led to a wider useable β range, it also introduced undesirable local minima in the Ixy profiles in the specified β range. The magnitudes and frequencies of the local minima were particularly sensitive to the *b* value. For *b* equal to 0.33, 0.25, and 0.20, the magnitudes of the lowest local minima were ~0.80, ~0.75, and ~0.60, respectively. However, despite this unwanted property, these short composite pulses had impressive β ranges that were superior to those of the β pulse or $\beta_{-60}(2\beta)_{60}$ composite pulse.

2.3. Conversion of short composite pulses into J-compensated sequences

A summary of short composite pulses derived in this paper, the resulting *J*-compensated sequences and their efficiencies is presented in Table 1. The creation of *J*-compensated sequences from composite pulses uses the formal analogy between transformation properties of the "RF pulse" operators {Ix, Iy, Iz} and "spin–spin coupling" operators {-2IxSz, 2IzSz, Iz} [7,9,10]. Basically, the RF pulse rotation of Iz magnetization for time t which can be represented by product operator transformation

$$I_z \overset{(\beta)I_x}{\rightarrow} I_z\cos\beta - I_y\sin\beta \qquad (1)$$

where $\beta = \gamma\ B_1 t$ is analogous to spin–spin *J*-coupling evolution (operator 2IzSz) of Iy for a delay τ represented by

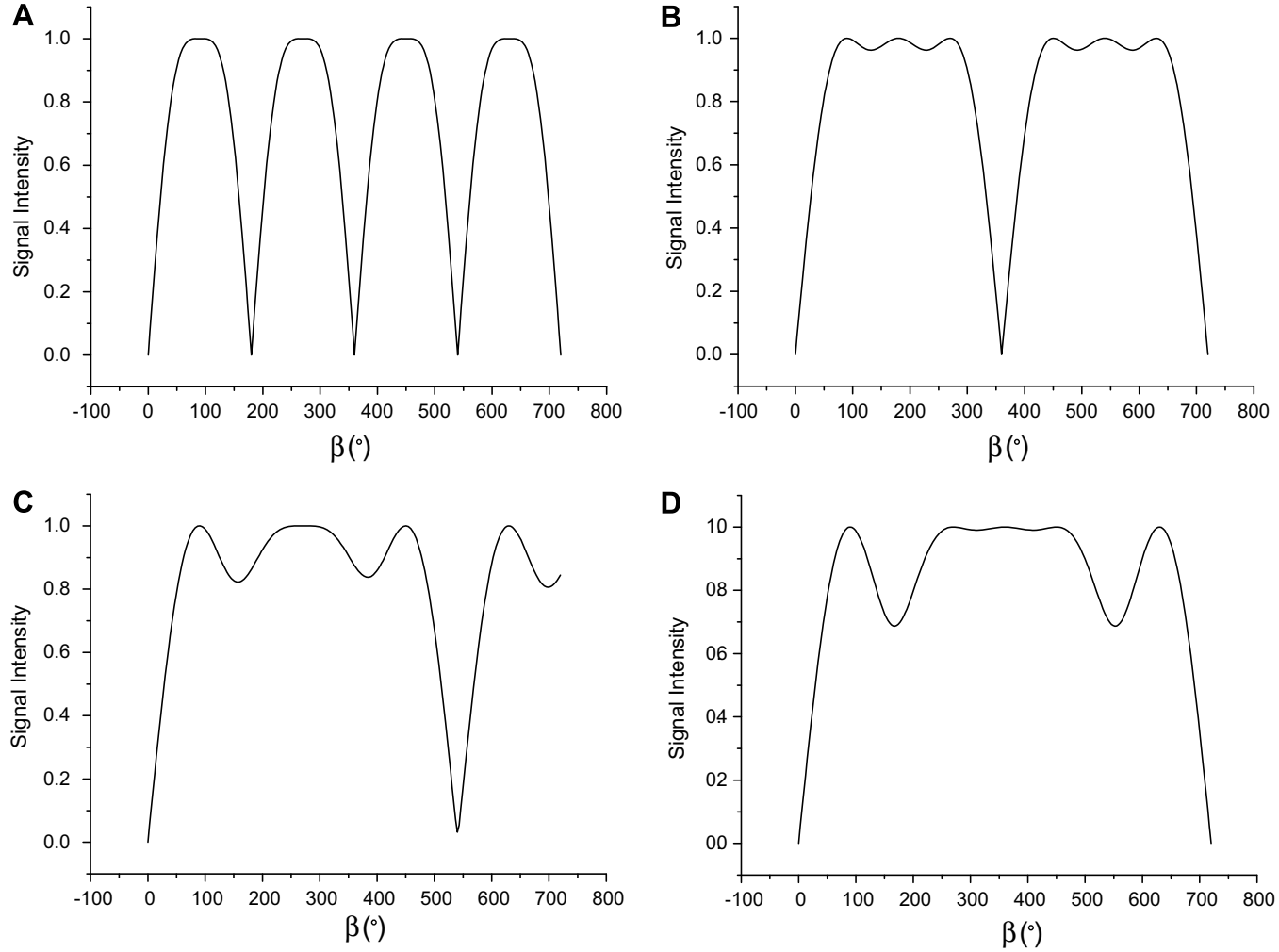

Fig. 2. Optimization of conversion of Iz to Ixy (as indicated by the relative signal intensity) by a composite pulse of the form $(\beta)_0(b\beta)_\varphi$. (A) $(\beta)_0\,(\beta)_{90}$; (B), $(\beta)_0(0.5\beta)_{90}$; (C) $(\beta)_0(0.33\beta)_{90}$; and (D) $(\beta)_0(0.25\beta)_{90}$.

Table 1
Summary of optimized short composite pulses and *J*-compensated experiments

RF pulse type	Alternative RF pulse name	*J*-compensated sequence	Relative duration	Number of local minima	Effective β range (conversion $\geqslant$ 0.7)
I. Conversion of Iz to Iy					
β_0	90_x	–	1.00	0	45–135°
$(0.5\beta)_{-60}(\beta)_{60}$	$45_x90_{(x+120)}$	*J*45 + 90A	1.50	0	62–298°
$0.5(\beta)_{-45}(\beta)_{45}$	$45_x90_{(x+90)}$	*J*45 + 90B	1.50	1	43–317°
II. Conversion of Iz to Ix + Iy					
$(\beta)_0(\beta)_{90}$	90_x90_y	*J*90 + 90	2.00	0	33–147°
$(\beta)_0\ 0.5(\beta)_{90}$	90_x45_y	*J*90 + 45	1.50	2	41–319°
$(\beta)_0\ 0.33(\beta)_{90}$	90_x30_y	*J*90 + 30	1.33	2	43–497°
$(\beta)_0\ 0.25(\beta)_{90}$	90_x22_y	*J*90 + 22	1.25	4	42–678°($\geqslant$0.68)

$$I_y \overset{(\beta')2I_zS_z}{\rightarrow} I_y\cos\beta' - 2I_xS_z\sin\beta' \tag{2}$$

where $\beta' = \pi J_{IS}\tau$. In short, an RF pulse of duration t is analogous to the spin–spin *J*-coupling delay τ. In many existing heteronuclear pulse experiments, the *J*-coupling delay τ is normally implemented with chemical shift refocusing pulses applied on both nuclei I and S and this can be represented by

$$-\tau/2 - 180^\circ{}_{90}(I,S) - \tau/2 - . \tag{3}$$

A composite pulse that efficiently converts Iz to −Iy can therefore be used to create a *J*-compensated sequence that converts Iy to −2IxSz while a composite pulse that efficiently converts Iz to transverse magnetization, Ix and Iy (Ixy), can be used in a *J*-compensated sequence that converts Iy to −2IxSz and 2IzSz. Details of the analogy and conversion procedure are described elsewhere [4,7] and they are not shown here.

2.4. J-compensated conversion of Iy to −2IxSz

Efficiently compensated sequences for converting Iy to −2IxSz can be derived by adopting the approach used for *J*-compensation of the DEPT sequence, particularly DEPTC1 [7]. This unusual *J*-compensated sequence starts with a 30° RF pulse instead of a 90° RF pulse, allowing the retention of a significant component of *z*-magnetization; thus there is a reduced probability of relaxation artifacts. In addition, DEPTC1 has no chemical shift refocusing pulses during the second delay, making it less sensitive to RF pulse-calibration imperfections.

The *J*-compensated sequence used for DEPTC1 was based on Levitt's $\beta_{-60}(2\beta)_{60}$ (or $\beta_x(2\beta)_{x+120}$) pulse and may be written as

$$60^\circ{}_{180} - 2\tau - 120^\circ{}_0 - \tau \tag{4}$$

where τ is the delay used to allow evolution of magnetization due to spin–spin coupling which is nominally set to $1/2J_{IS}$ and RF pulses are applied to spin I only. The 60° and 120° RF pulses on spin I in DEPTC1, and their corresponding phases, are dependent on the phase shifts of the incorporated composite pulses. The above sequence provides *J*-compensated conversion of Iy to −2IxSz or −Iy to 2IxSz. By analogy, for $(0.5\beta)_{-60}\,(\beta)_{60}$ (whose duration is half that of $\beta_{-60}(2\beta)_{60}$) the *J*-compensated sequence is:

$$60^\circ_{180} - \tau - 120^\circ_0 - 0.5\tau. \tag{5}$$

For the $(0.5\beta)_{45}\,(\beta)_{-45}$ composite pulse, the resulting compensated sequence that will be obtained after proper conversion is

$$45^\circ{}_{180} - \tau - 90^\circ{}_0 - 0.5\tau. \tag{6}$$

We refer to these two *J*-compensated sequences in Eq. (5) and (6) as *J*45 + 90A and *J*45 + 90B, respectively (see Table 1). These two compensated sequences which efficiently convert Iy to −2IxSz may be appended after the $90^\circ{}_0$ excitation pulse on spin I to create *J*-compensated sequences that transform longitudinal magnetization Iz to 2IxSz:

$$90^\circ{}_0 - 60^\circ{}_{180} - \tau - 120^\circ{}_0 - 0.5\tau \equiv 30^\circ{}_0 - \tau - 120^\circ{}_0 - 0.5\tau \tag{7}$$

and

$$90^\circ{}_0 - 45^\circ{}_{180} - \tau - 120^\circ{}_0 - 0.5\tau \equiv 45^\circ{}_0 - \tau - 90^\circ{}_0 - 0.5\tau. \tag{8}$$

Clearly, these two compensated sequences can be used to replace the first part of many experiments that require creation of antiphase magnetization. Compared with the conventional HMBC [16,20] (Fig. 3A), the *J*-compensated sequences, referred to as HMBC-*J*45 + 90A and HMBC-*J*45 + 90B (Fig. 3B), are unusual in that the first pulses are less than 90° and the second delay 0.5 τ does not incorporate a chemical shift refocusing pulse. The omission of a refocusing pulse is made possible by the fact that the HMBC sequence in itself does not require refocusing during the delay τ. These improvements in the *J*-compensated HMBC sequence are similar to those in DEPTC1 except that the 120° pulse is phase-shifted by 180°, since the proton refocusing pulse in the first delay is phase-shifted by 90°.

2.5. J-compensated conversion of Iy to −2IxSz and −2IySz

As noted above, a composite pulse for the conversion of Iz to Ixy can be used to create a *J*-compensated conversion of Iy to −2IxSz and 2IzSz. The popular $(\beta)_0(\beta)_{90}$ composite pulse when transformed into a *J*-compensated sequence is given by:

$$\tau - 90^\circ{}_{270} - \tau. \tag{9}$$

To use this sequence for HMBC, it is necessary to consider that the first delay, τ, in the conventional HMBC sequence does not include a chemical shift refocusing pulse, so that the resulting magnetization prior to the first 90° pulse on S is applied to a linear combination of antiphase magnetizations, 2IxSz and 2IySz. Both of these components contribute to the measured signal, so in order to be quantitative the data are only processed in magnitude mode in f_2. The 2IzSz component produced by the compensated sequence can be converted selectively to −2IySz by a $90^\circ{}_0$ pulse on spin I. Thus the resulting sequence is:

$$\tau - 90^\circ{}_{270} - \tau - 90^\circ{}_0. \tag{10}$$

For any composite pulse of the form $(\beta)_0(b\beta)_{90}$, the corresponding *J*-compensated sequence is:

$$\tau - 90^\circ{}_{270} - b\tau - 90^\circ{}_0. \tag{11}$$

The resulting *J*-compensated HMBC sequences based on Eq. (10) are referred to as HMBC-*J*90 + 90, while those based on Eq. (11) for $b = 0.5$, 0.33 and 0.25 are referred to as HMBC-*J*90 + 45, HMBC-*J*90 + 30 and HMBC-*J*90 + 22, respectively. These pulse sequences are depicted in Fig. 4C. Note that unlike the two sequences based on Eq. (7) and (8), these sequences start with a $90^\circ{}_0$ pulse on I and incorporate additional refocusing pulses during the second delay. As a result, they are expected to be more prone to the deleterious effects of relaxation and imperfections in pulse calibration.

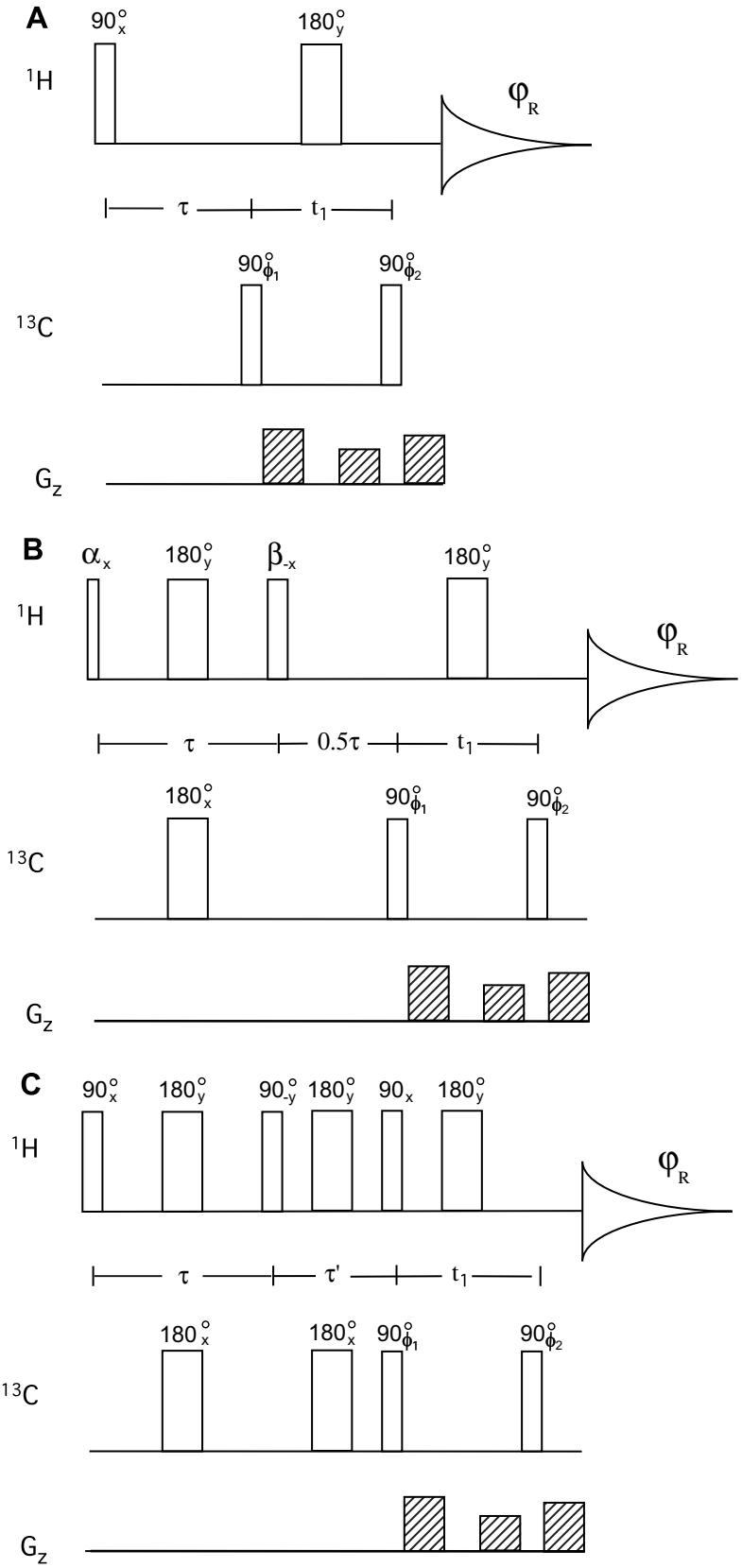

Fig. 3. Pulse sequences for conventional and *J*-compensated HMBC experiments. (A) conventional HMBC; (B) HMBC-*J*45 + 90A ($\alpha = 30°$, $\beta = 120°$), HMBC-*J*45 + 90B ($\alpha = 45°$, $\beta = 90°$); and (C), HMBC-*J*90 + 90 ($\tau' = \tau$), HMBC-*J*90 + 45 ($\tau' = 0.5\tau$), HMBC-*J*90 + 30 ($\tau' = 0.33\tau$), and HMBC-*J*90 + 22 ($\tau' = 0.25\tau$). The delay τ is normally set to ~80 ms to observe long-range CH correlations. Here, τ was set to 78 ms to illustrate the effectiveness of the newly derived sequences on sodium acrylate. The gradient ratios were 50:30:40 as normally implemented in the gradient version of HMBC [20] to select double-quantum coherences. ϕ_1 = x − x x −x; ϕ_2 = x x− x−x; and φ_R = x −x −x x.

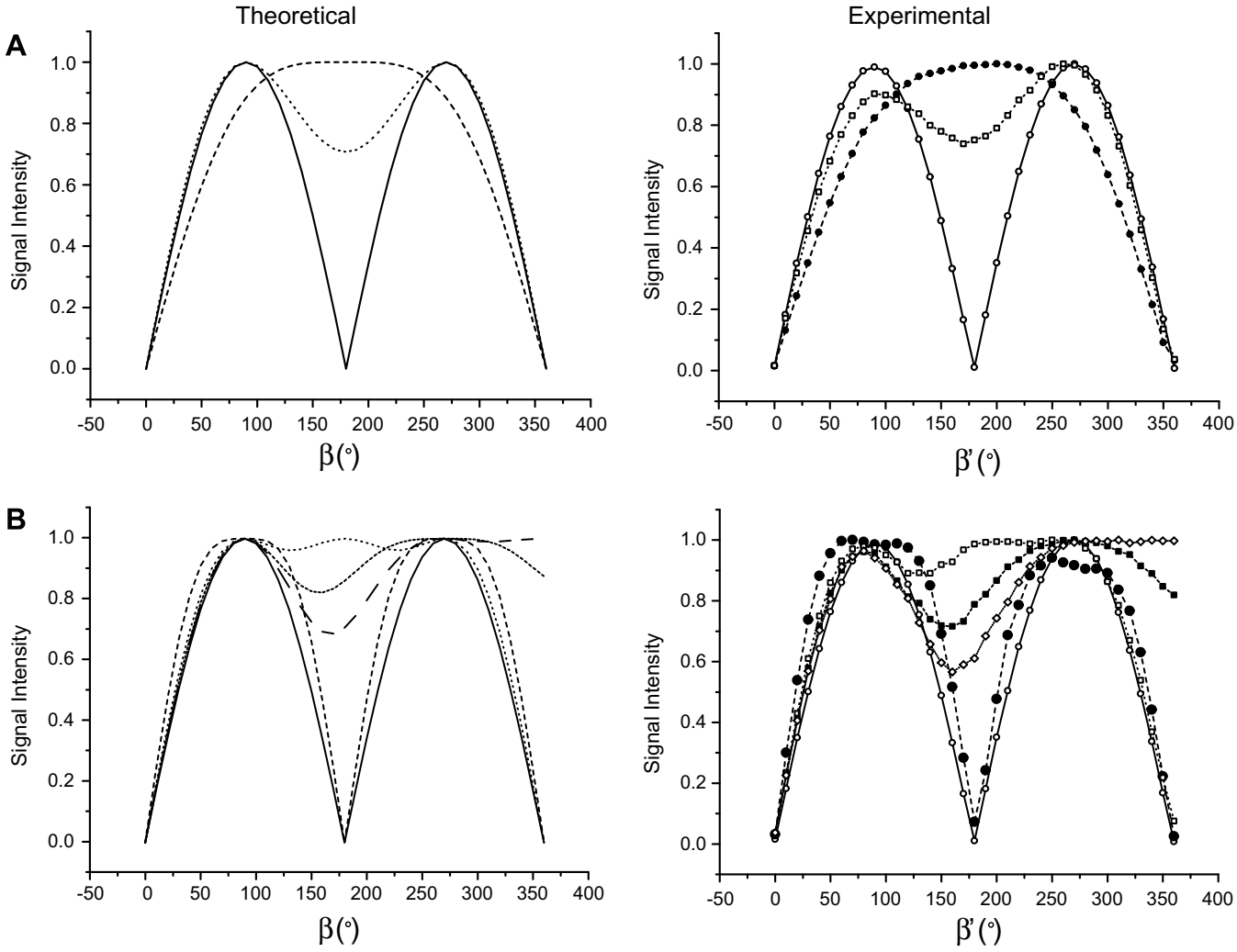

Fig. 4. Theoretical and experimental performance of regular and *J*-compensated sequences as indicated by the relative signal intensity. Antiphase magnetization profiles for $CHCl_3$ were created from evolution of in-phase proton magnetization due to direct CH *J*-coupling using the HMBC pulse sequences presented in Fig. 3. Note that in all HMBC experiments, the τ delay was set for direct coupling ($^1J_{CH}$ = 209.3 Hz) instead of long-range coupling. (A) conventional HMBC (solid line), HMBC-*J*45 + 90A (dashed line), HMBC-J45 + 90B (dotted line). (B) conventional HMBC (solid line), HMBC-*J*90 + 90 (long dashed line), HMBC-*J*90 + 45 (dotted line), HMBC-*J*90 + 30 (short dashed line) and HMBC-*J*90 + 22 (broken solid line).

3. Experimental

NMR experiments were performed on a Bruker DRX-600 spectrometer equipped with a 5-mm triple resonance ($^1H/^{13}C/^{15}N$) cryoprobe with *z*-gradient coil; the variable temperature unit was set to 298 K. The conventional HMBC pulse sequence with 4-step phase cycle and gradient coherence selection (as shown in Fig. 3) was used as a template for the *J*-HMBC sequences. No low-pass *J*-filters or purging sequences, that reduce signal due to one-bond correlations, were implemented. The gradient ratio employed for all HMBC and *J*-compensated sequences was 50:30:40 of maximum *z*-gradient of 70 G cm^{-1}. The 90° pulse was typically 8 μs for ^1H and 15 μs for ^{13}C. Sample compounds were 20% (v/v) $CHCl_3$ in $CDCl_3$ and 50 mg sodium acrylate (**1**; Fig. 5) in 0.5 mL D_2O. Experimental signal-intensity profiles of different *J*-compensated sequences were obtained using 1D versions of HMBC and employing a $CHCl_3$ sample in $CDCl_3$. The τ delay was varied to cover the range up to $\beta' = \pi J\tau$ where $^1J_{CH}$ = 209.3 Hz.

For experiments on sodium acrylate, 2D data sets consisted of 512 points × 64 increments covering spectral widths of 2003 Hz (^1H) and 13583 Hz (^{13}C). Four dummy scans were used prior to acquisition, and four transients were collected per t_1 increment. Data sets were apodized with a cosine function in both dimensions and zero-filled to obtain a final data matrix of 1024 × 512. For the reasons noted above, all spectral data were processed in magnitude mode.

4. Results and discussion

4.1. Signal-intensity profiles of short composite pulses and *J*-compensated sequences

Fig. 4 shows theoretical and experimental signal-intensity profiles obtained with the RF pulses and *J*-compensated sequences given in Fig. 3 and Table 1. The theoretical intensity profiles are presented for each sequence as a function of β, while the experimental profiles are shown for HMBC and corresponding *J*-compensated HMBC sequences as a function of β' Note that the experimental HMBC signal-intensity profiles were obtained by measuring antiphase proton CH signal intensity from $CHCl_3$ for which β' or τ were set values relevant to the direct CH coupling ($^1J_{CH}$ = 209.3 Hz). For all cases, there was good agreement between the theoretical and experimental profiles.

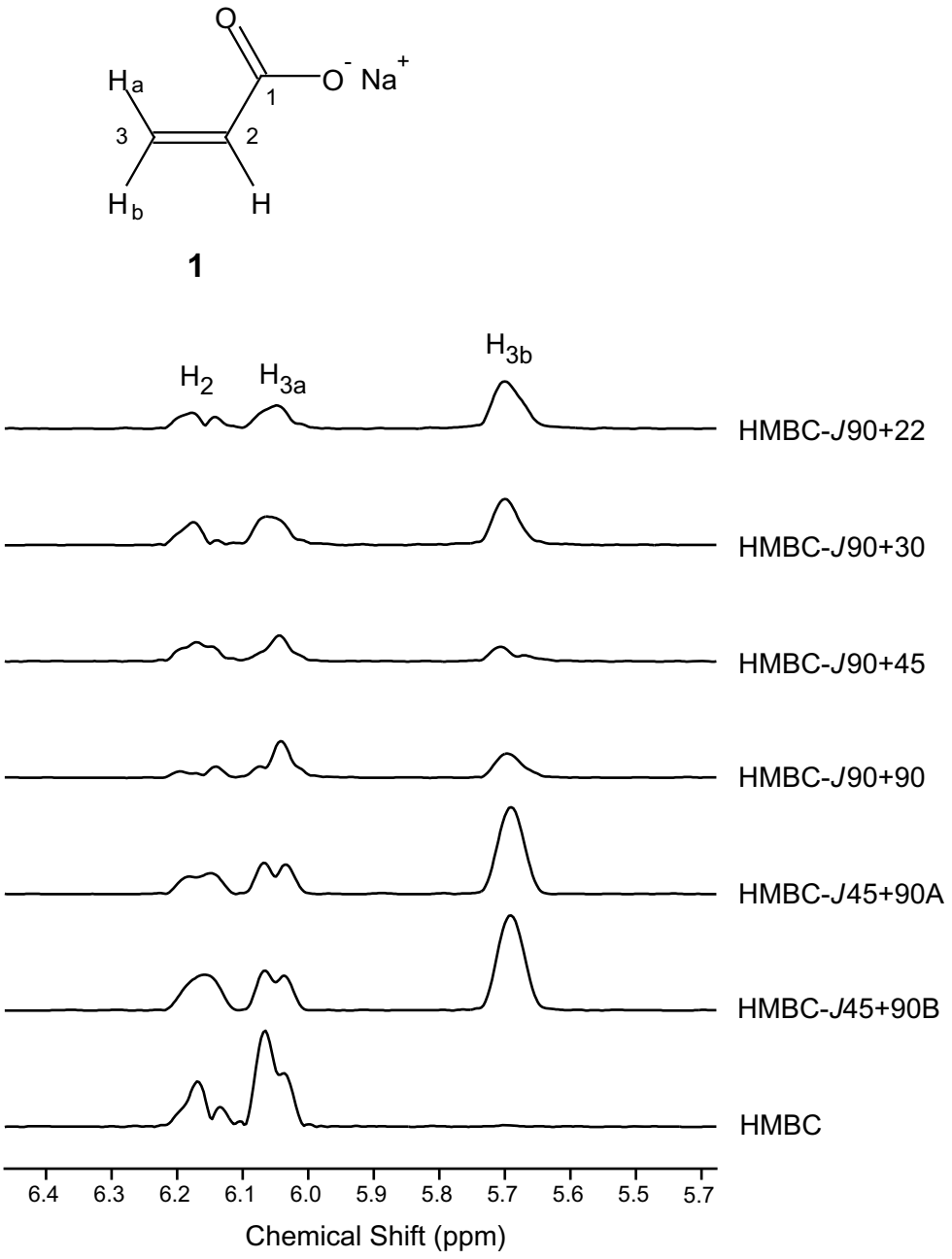

Fig. 5. Selected F_2 slices from 2D maps of HMBC and *J*-compensated HMBC experiments with sodium acrylate (**1**). Each slice was obtained from the carboxyl carbon (C-1) cross-peak of the relevant spectrum. The F_2 slices are plotted at the same absolute intensity.

For the conversion of Iy to −2IxSz, the HMBC-*J*45 + 90A sequence that was based on $(0.5\ \beta)_{-60}(\beta)_{60}$ provided a broader signal profile than the regular sequence, yielding a maximum value for $\beta' = 180°$ where the conventional method yielded almost no signal. A disadvantage of this compensated sequence is that the signals at $\beta' = 90°$ and 270° are ~90% of those obtained with the conventional sequence. The HMBC-*J*45 + 90B sequence based on $(0.5\beta)_{-45}(\beta)_{45}$, on the other hand, produced an excitation envelope of comparable width to the regular sequence. There was a local minimum at $\beta' = 180°$ but its intensity remained ~75% of the maximum while performance at regions near $\beta' = 90°$ and 270° was basically identical to that of the conventional RF pulse sequence. There were slight asymmetries in the experimental profiles of some *J*-compensated sequences; this could be attributed to small RF pulse imperfections and relaxation effects, as *J*-compensated schemes include more RF pulses and delays than their conventional HMBC counterparts.

The performance of the *J*-compensated sequences for the conversion of Iy to −2IxSz and −2IySz was *very impressive* especially for HMBC-*J*90 + 45, HMBC-*J*90 + 30, and HMBC-*J*90 + 22 which all yielded significant signal at $\beta' \sim 180°$. Of the three sequences, HMBC-*J*90 + 22 yielded the smallest signal in this region but its signal at $\beta' \sim 360°$ was the largest. All profiles at $\beta' \sim 90°$ were similar to that obtained with the single delay τ in the conventional HMBC sequence. HMBC-*J*90 + 90 provided broader signal profiles for most β' regions but its signal at $\beta' \sim 180°$ was only marginally higher than that of the conventional HMBC sequence. A more detailed comparison of the theoretical and experimental profiles showed that the minima obtained for the *J*-compensated sequences (exper-

imental) are slightly deeper than expected. Again, this discrepancy could most likely be attributed to imperfections in the calibration of the RF pulses, and to relaxation effects.

4.2. J-compensated HMBC experiments

The new HMBC sequences were evaluated using sodium acrylate (**1**; Fig. 5) as a test sample. This compound was chosen because it displays a wide range of J_{CH} values to the carboxyl carbon and appreciable proton–proton coupling [19]. Fig. 5 presents C1 slices obtained from the regular, and *J*-compensated, HMBC experiments where $\tau = 78$ ms (nominally set to yield maximum intensity, i.e., $\beta' = 90°$ for $J_{CH} = 6.4$ Hz). With this value, C1-H2 and C1-H3a correlations were visible in regular HMBC experiments but the C1-H3b ($^3J_{C1\text{-}H3b} = 14.1$ Hz; $\beta' \sim 180°$) was clearly absent. All *J*-compensated sequences yielded spectra with this correlation although its intensity varied for each method.

HMBC-*J*45 + 90A and HMBC-*J*45 + 90B experiments both yielded similar spectra with very strong C1-H3b correlations, in fact they were even more intense than those for C1-H2 and C1-H3a. As compared with the regular HMBC sequence, these two *J*-compensated sequences provided C1-H2 correlations that had comparable magnitudes, while the C1-H3a correlations were slightly smaller.

The remaining *J*-compensated experiments, HMBC-*J*90 + 90, HMBC-*J*90 + 45, HMBC-*J*90 + 30, and HMBC-*J*90 + 22, provided significant C1-H3b correlations although not as intense as those of the HMBC-*J*45 + 90A and HMBC-*J*45 + 90B sequences. It was also apparent that the C1-H2 and C1-H3a peaks were smaller than those obtained from the regular HMBC and other compensated sequences. The additional delay and pulses in this group of sequences could easily account for the decrease in signal. We have shown previously [19] that unwanted homonuclear coupling during the extra delay may decrease signal intensity in *J*-compensated sequences.

5. Conclusions

We have described the process of developing short *J*-compensated sequences that are useful for wide range of experiments such as HMBC. These compensated sequences are desirable as their duration is extended by only $\leqslant$50% compared with conventional experiments. Of the various *J*-compensated HMBC experiments investigated, HMBC-*J*45 + 90A and HMBC-*J*45 + 90B, which are based on $(0.5\beta)_{-60}(\beta)_{60}$ and $(0.5\beta)_{-45}(\beta)_{45}$, respectively, were more effective over a wider range of $^nJ_{CH}$ values and they were less prone to pulse-calibration imperfections. These two experiments are unusual in that their pulse sequences start with an RF pulse of less than 90°. *J*-compensated HMBC experiments based on $(\beta)_0(0.5\beta)_{90}$, $(\beta)_0(0.33\beta)_{90}$, and $(\beta)_0(0.25\beta)_{90}$ displayed some broadband characteristics but suffered from diminished overall signal intensity, presumably due to relaxation losses that are associated with such lengthy pulse sequences.

Acknowledgments

We thank Mr. Bill Lowe for technical assistance. The work was supported by an Australian Research Council Discovery Grant to P.W.K. and Dr J.I. Vandenberg.

References

[1] R. Freeman, S.P. Kempsell, M.H. Levitt, Radiofrequency pulse sequences which compensate their own imperfections, J. Magn. Reson. 38 (1980) 453–479.
[2] M.H. Levitt, R. Freeman, NMR population inversion using a composite pulse, J. Magn. Reson. 33 (1979) 473–476.
[3] H. Geen, R. Freeman, Band-selective radiofrequency pulses, J. Magn. Reson. 93 (1991) 93–141.
[4] S. Wimperis, G. Bodenhausen, Heteronuclear coherence transfer over a range of coupling constants. A broadband-INEPT experiment, J. Magn. Reson. 69 (1986) 264–282.
[5] T.M. Barbara, R. Tycko, D.P. Weitekamp, Composite sequences for efficient double-quantum excitation over a range of spin coupling strengths, J. Magn. Reson. 62 (1985) 54–64.
[6] S. Wimperis, Broadband and narrowband composite excitation sequences, J. Magn. Reson. 86 (1990) 46–59.
[7] A.M. Torres, R.E.D. McClung, *J*-compensated DEPT sequences, J. Magn. Reson. 92 (1991) 45–63.
[8] G.C. Chingas, A.N. Garroway, R.D. Bertrand, W.B. Moniz, Zero quantum NMR in the rotating frame: *J* cross polarization in AXN systems, J. Chem. Phys. 74 (1981) 127–156.
[9] A.M. Torres, R.E.D. McClung, T.T. Nakashima, Compensated APT pulse sequences, J. Magn. Reson. 87 (1990) 189–193.
[10] A.M. Torres, T.T. Nakashima, R.E.D. McClung, Improved *J*-compensated APT experiments, J. Magn. Reson. A 101 (1993) 285–294.
[11] A.M. Torres, T.T. Nakashima, R.E.D. McClung, *J*-compensated proton-detected heteronuclear shift-correlation experiments, J. Magn. Reson. A 102 (1993) 219–227.
[12] D.J. Philp, P.W. Kuchel, A way of visualizing NMR experiments on quadrupolar nuclei, Concepts Magn. Reson. A 25 A (2005) 40–52.
[13] M.H. Levitt, Symmetrical composite pulse sequences for NMR population inversion. I. Compensation of radiofrequency field inhomogeneity, J. Magn. Reson. 48 (1982) 234–264.
[14] O.W. Sorensen, J.C. Madsen, N.C. Nielsen, H. Bildsoe, H.J. Jakobsen, An improved refocused INEPT experiment. Application for sensitivity enhancement and spectral editing in carbon-13 NMR, J. Magn. Reson. 77 (1988) 170–174.
[15] N.C. Nielsen, H. Bildsoe, H.J. Jakobsen, O.W. Soerensen, Composite refocusing sequences and their application for sensitivity enhancement and multiplicity filtration in INEPT and 2D correlation spectroscopy, J. Magn. Reson. 85 (1989) 359–380.
[16] A. Bax, M.F. Summers, Proton and carbon-13 assignments from sensitivity-enhanced detection of heteronuclear multiple-bond connectivity by 2D multiple quantum NMR, J. Am. Chem. Soc. 108 (1986) 2093–2094.
[17] A. Bax, R.H. Griffey, B.L. Hawkins, Correlation of proton and nitrogen-15 chemical shifts by multiple quantum NMR, J. Magn. Reson. 55 (1983) 301–315.
[18] K. Furihata, H. Seto, Decoupled HMBC (D-HMBC), an improved technique of HMBC, Tetrahedron Lett. 36 (1995) 2817–2820.
[19] A.M. Torres, W.A. Bubb, P.W. Kuchel, Experiments to detect long-range heteronuclear shift correlations: LR-J-HSMQC, J. Magn. Reson. 156 (2002) 249–257.
[20] W. Willker, D. Leibfritz, R. Kerssebaum, W. Bermel, Gradient selection in inverse heteronuclear correlation spectroscopy, Magn. Reson. Chem. 31 (1993) 287–292.